Tetrahedron 65 (2009) 8104–8112

Contents lists available at ScienceDirect

Tetrahedron

journal homepage: www.elsevier.com/locate/tet

Synthesis, structures, and properties of peripheral *o*-dimethoxy-substituted pentiptycene quinones and their *o*-quinone derivatives

Jing Cao [a,b], Hai-Yan Lu [b], Chuan-Feng Chen [a,*]

[a] Beijing National Laboratory for Molecular Sciences, CAS Key Laboratory of Molecular Recognition and Function, Institute of Chemistry, Chinese Academy of Sciences, Beijing 100190, China
[b] Graduate School, Chinese Academy of Sciences, Beijing 100049, China

ARTICLE INFO

Article history:
Received 15 June 2009
Received in revised form 24 July 2009
Accepted 30 July 2009
Available online 6 August 2009

Keywords:
Pentiptycene quinones
Synthesis and structure
Self-assembly in the solid state
Photo-physical property
Electrochemistry property

ABSTRACT

A series of peripheral *o*-dimethoxy-substituted pentiptycene quinones and their *o*-quinone derivatives have been synthesized. Especially, it was found that if two *o*-dimethoxybenzene moieties were situated at the same side of the pentiptycene quinones, one of them was only oxidized by excess CAN in aqueous acetonitrile. Moreover, the pentiptycene quinones with unique 3D rigid structure could all self-assemble into a 3D microporous structure in the solid state. For the pentiptycene quinones containing the dimethoxybenzene unit(s) and the quinone group(s) simultaneously, interesting intramolecular charge transfer interactions and electrochemical properties were also shown. These peripheral-substituted pentiptycene quinones and their *o*-quinone derivatives can be used as new useful building blocks and will find wide applications in material science and host–guest chemistry.

1. Introduction

Pentiptycene and its derivatives are a class of structurally unique compounds consisting of five arenes that are fused together through the bicycle[2.2.2]octane framework, and they all possess a rigid, aromatic, and H-shaped scaffold.[1] Such a structural feature has made them to be promising reagents for the preparation of porous films with bright luminescence for π-conjugated polymers,[2] fluorescent porous polymeric sensors for TNT,[2b,3] fluorescent chemosensors for Cu^{2+},[4] materials with monolayer assembly structures,[5] light-driven molecular brake,[6] electron donor porphyrin quinone diads and triads,[7] and building blocks for the construction of novel chain and channel networks.[8] However, it was noted that these applications were almost based on the central-ring functionalized pentiptycenes. Although the peripheral functionalized pentiptycene derivatives, such as peripheral *o*-dimethoxy-substituted pentiptycenes and their *o*-quinone derivatives could be used as new useful building blocks, and subsequently found wide applications in material science and supramolecular chemistry,[9] few are so far known about them.

Pentiptycene quinones refer to the pentiptycene derivatives bearing at least one benzoquinone unit. They have attracted much interest during the past decade for their unique structural feature of pentiptycene and specific electrochemical and photochemical properties of quinone. Although some different synthetic methods[2,10] for pentiptycene quinones have been developed, they proceeded in multi-step routes or unsatisfactory yields. Recently, we developed a practical and efficient method for the synthesis of iptycene quinones including pentiptycene quinones.[11] In this paper, we report (1) the synthesis of a series of peripheral *o*-dimethoxy-substituted pentiptycene quinones and their *o*-quinone derivatives, (2) their self-assemblies in the solid state, and (3) their optical and electrochemical properties.

2. Results and discussion

2.1. Synthesis of peripheral *o*-dimethoxy-substituted pentiptycene quinones

Triptycene monoquinones **4**,[12] **5**,[13] and **6** were prepared by the reaction of anthracene **1**, 2,3-dimethoxyanthracene **2**[14] or 2,3,6,7-tetramethoxyanthracene **3**[14a] with excess *p*-benzoquinone in acetic acid in an one-pot approach, respectively. As compound **3** has a poor solubility in refluxing acetic acid, 1,2-dichloroethane was then used as the co-solvent to improve its solubility in the solution.

* Corresponding author. Tel.: +86 10 62588936; fax: +86 10 62554449.
E-mail address: cchen@iccas.ac.cn (C.-F. Chen).

0040-4020/$ – see front matter © 2009 Elsevier Ltd. All rights reserved.
doi:10.1016/j.tet.2009.07.090

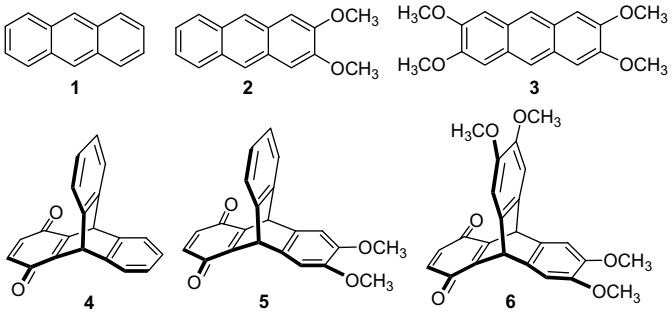

We recently reported that the reaction of triptycene quinone **4** with anthracene **1** in acetic acid in the presence of *p*-chloranil could give pentiptycene quinone **7** in 78% yield.[11] According to the similar reaction conditions, a series of peripheral *o*-dimethoxy-substituted pentiptycene quinones have been synthesized. Firstly, pentiptycene quinone **8** with one *o*-dimethoxybenzene unit was obtained in 75% yield by the reaction of triptycene quinone **4** with 2,3-dimethoxyanthracene **2** or the reaction of anthracene **1** with triptycene quinone **5** in refluxing acetic acid in the presence of *p*-chloranil. The ^{1}H NMR spectrum of **8** showed two singlets for the bridgehead protons (δ 5.75, 5.67) and one singlet for the methoxyl protons (δ 3.79). Its ^{13}C NMR spectrum showed two peaks for the bridgehead carbons (δ 47.5, 47.2), one peak for the methoxyl carbons (δ 56.3), and one peak for the carbonyl carbons (δ 180.0).

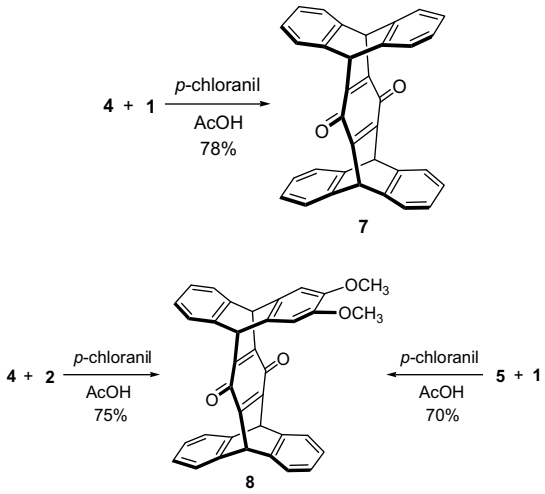

The reaction of triptycene quinone **4** with 2,3,6,7-tetramethoxyanthracene **3** in a mixture of acetic acid and 1,2-dichloroethane in the presence of *p*-chloranil gave pentiptycene quinone **9** in only 10% yield even after we prolonged the reaction time to more than one week. But we found that when the reaction of anthracene **1** and triptycene quinone **6** took place in refluxing acetic acid in the presence of *p*-chloranil, **9** could be achieved in 89% yield. The ^{1}H NMR spectrum of **9** showed two singlets for the bridgehead protons (δ 5.75, 5.58) and one singlet for the methoxyl protons (δ 3.79). In its ^{13}C NMR spectrum, two peaks for the bridgehead carbons (δ 47.5, 46.9), one peak for the methoxyl carbons (δ 56.3), and one peak for the carbonyl carbons (δ 180.1) were shown.

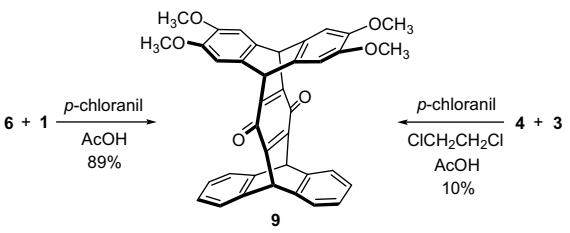

Under the same reaction conditions as described above, the reaction of dimethoxyanthracene **2** with triptycene quinone **5** gave a mixture of two isomers **10a** and **10b** in 85% of total yield, which could be easily separated by column chromatography. It was found that compared with **10a**, the isomer **10b** with two *o*-dimethoxylbenzene moieties in the trans position has smaller polarity and poorer solubility in dichloromethane. The isomers **10a** and **10b** showed almost the same ^{1}H NMR spectra (one singlet for the bridgehead protons, one singlet for the *o*-dimethoxyl protons, and one singlet and two 4-proton multiplets for the aryl protons) and ^{13}C NMR spectra (one peak for the bridgehead carbons, one peak for the carbonyl carbons, one peak for the methoxyl carbons, and seven peaks for the aromatic carbons), and they could not be distinguished by ordinary spectroscopic methods. Fortunately, we obtained the single crystals of the isomers. The results of X-ray crystal structure analyses expectedly showed that the two *o*-dimethoxylbenzene moieties in **10a** are in the cis position, while they are in the trans position in **10b** (Fig. 1).

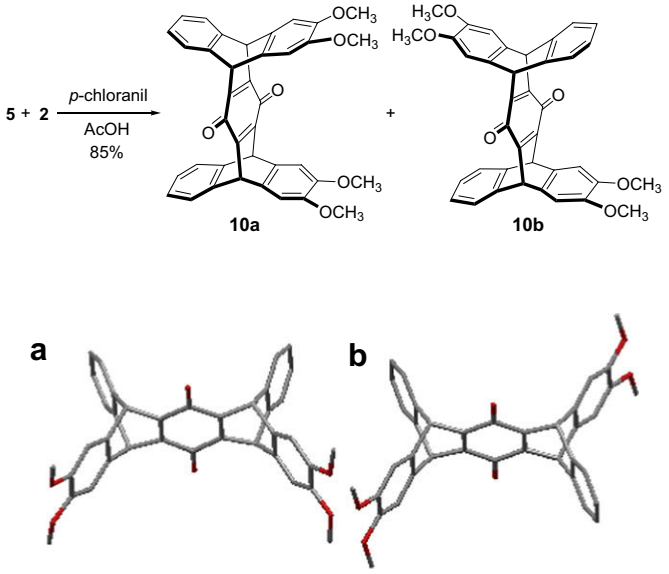

Figure 1. Crystal structures of (a) **10a**, and (b) **10b**. Solvent molecules and hydrogen atoms were omitted for clarity.

Similar to the case of **9**, pentiptycene quinone **11** has been synthesized in only 10% yield by the reaction of triptycene quinone **5** with 2,3,6,7-tetramethoxyanthracene **3** in acetic acid and 1,2-dichloroethane in the presence of *p*-chloranil, but could be obtained in 75% yield by the reaction of **6** and 2,3-dimethoxyanthracene **2** in acetic acid in the presence of *p*-chloranil. In the ^{1}H NMR spectrum of **11**, two singlets for the bridgehead protons (δ 5.67, 5.59), one singlet for the *o*-dimethoxyl protons (δ 3.79) were observed. Its ^{13}C NMR spectrum showed two peaks for the bridgehead carbons (δ 47.2, 46.9), one peak for the methoxyl carbons (δ 56.4), and one peak for the carbonyl carbons (δ 180.1).

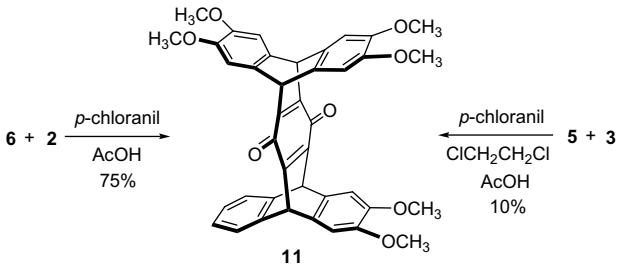

It was found that no reaction occurred between triptycene quinone **6** and 2,3,6,7-tetramethoxyanthracene **3** in refluxed acetic acid in the presence of *p*-chloranil probably due to the poor solubility of **3**. But when 1,2-dichloroethane was used as the co-solvent, pentiptycene quinone **12** could be obtained in 16% yield after a week. In the ^{1}H NMR spectrum of **12**, one singlet for the bridgehead protons (δ 5.59), one singlet for the aromatic protons (δ 6.97), and one singlet for the *o*-dimethoxyl protons (δ 3.79) were observed. Moreover, its ^{13}C NMR showed only one peak for the bridgehead carbons (δ 46.9), one peak for the *o*-dimethoxyl carbons (δ 56.3), one peak for the carbonyl carbons (δ 180.2), and four peaks for the aryl carbons. These observations were all consistent with its D_{2h} symmetry.

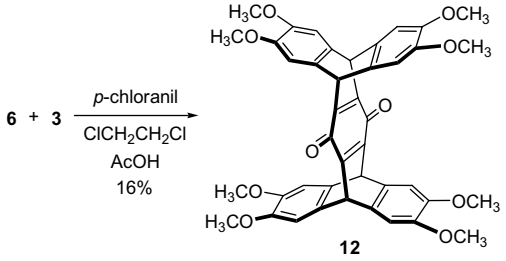

We have further tried one-pot approach for synthesis of some pentiptycene quinones with C_{2v} or D_{2h} symmetry. Consequently, it was found that when 2 equiv of anthracene **1** was reacted with 1 equiv of *p*-benzoquinone in acetic acid in the presence of 2 equiv of *p*-chloranil, pentiptycene quinone **7** could be directly achieved in 89% yield, which was higher than that of the reaction of **1** with triptycene quinone **4**. Similarly, one-pot reaction of 2,3-dimethoxyanthracene **2** with *p*-benzoquinone gave trans/cis isomers **10a**/**10b** in 85% of total yield. When the reaction of 2,3,6,7-tetramethoxyanthracene **3** with *p*-benzoquinone in refluxing acetic acid and 1,2-dichloroethane in the presence of *p*-chloranil occurred, we found that only a little product **12** was obtained, and major product was triptycene quinone **6**.

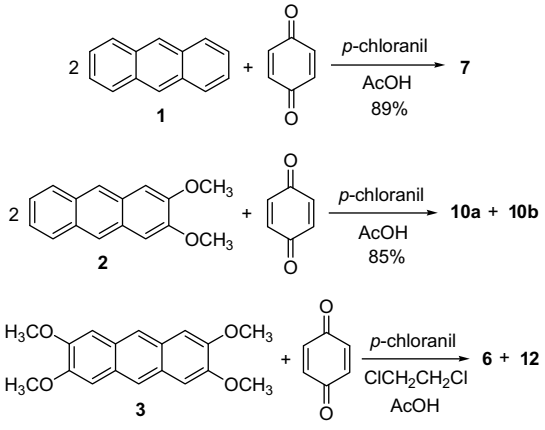

2.2. Synthesis of pentiptycene *o*-quinone derivatives

We first tested the reaction of 1 equiv of pentiptycene quinone **8** with 3 equiv of cerium ammonium nitrate (CAN) in aqueous acetonitrile,[15] and found that pentiptycene *o*-quinone **13** could be obtained in 94% yield. The ^{1}H NMR spectrum of **13** showed two singlets for the bridgehead protons (δ 5.43, 5.82), one singlet for the –C═CH protons of the quinoid ring (δ 6.33). In its ^{13}C NMR spectrum, two peaks for the bridgehead carbons (δ 47.5, 45.1) and two peaks for the carbonyl carbons (δ 178.9, 178.8) were observed.

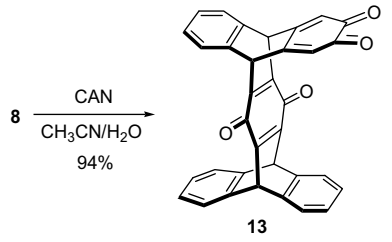

Under the same reaction conditions as above, pentiptycene *o*-quinone derivatives **14** and **15** could be obtained by the oxidation of the isomers **10a** and **10b** with CAN in aqueous acetonitrile, respectively. It was found that compound **15** with the two *o*-quinone moieties in the trans position showed smaller polarity and poorer solubility than those of **14** with the two *o*-quinone moieties in the cis position. Compounds **14** and **15** showed almost the same ^{1}H NMR spectra (one singlet for the bridgehead protons, one singlet for the C═CH protons of the quinoid rings and two 4-proton multiplets for the aryl protons). In the ^{13}C NMR spectrum of **14**, one peak for the bridgehead carbons (δ 44.1) and two peaks for the carbonyl carbons (δ 178.9, 179.0) were observed. As compound **15** has a poor solubility even in DMSO, we didn't obtain its ^{13}C NMR spectrum.

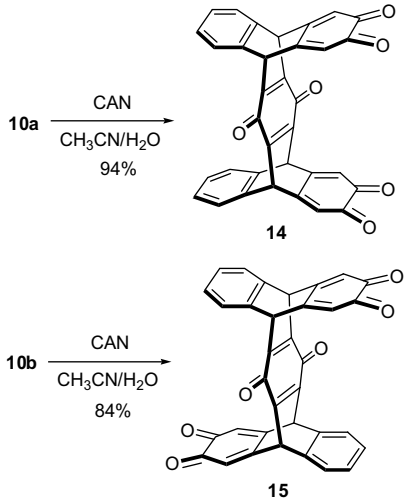

When the oxidation reaction of pentiptycene quinone **9** with 6 equiv CAN took place in aqueous acetonitrile, we found that compound **16** instead of pentiptycene bis(*o*-quinone) was only isolated in 80% yield. Moreover, it was found that **16** could not be further oxidized by large excess CAN in even long reaction time. The ^{1}H NMR spectrum of **16** showed one singlet for the methoxyl protons (δ 3.85), two singlets for the bridgehead protons (δ 5.82, 5.35), one singlet for the protons of the quinoid ring (δ 6.29), and one singlet for the aryl protons of the *o*-dimethoxybenzene ring (δ 6.93). In its ^{13}C NMR spectrum, two peaks for the bridgehead carbons (δ 47.6, 44.8), one peak for the methoxyl carbons (δ 56.3), and two peaks for the carbonyl carbons (δ 178.9, 179.1) were observed.

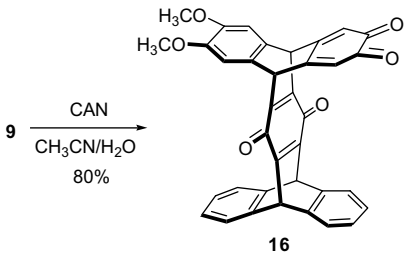

Similar to the case of **9**, one of the *o*-dimethoxybenzene moieties in pentiptycene quinone **11** could be only oxidized by CAN in aqueous acetonitrile to give two isomers **17a** and **17b** in 80% of total yield, which could be separated with a mixture of 50:1 (v/v) dichloromethane/ethyl acetate as eluent. The isomers showed almost the same ^{1}H NMR spectra (one singlet for the methoxyl protons, two singlets for the bridgehead protons, two singlets for the protons of the quinoid rings, and one singlet for the aryl protons of the *o*-dimethoxybenzene moiety), and they could not be distinguished by ordinary spectroscopic methods. We have also tried to get the single crystals of the isomers, but unfortunately unsucceeded. However, by comparing with the isomers **14** and **15**, we proposed that the isomer **17b** with smaller polarity and poorer solubility could have the two *o*-quinone moieties lying in the trans position, while in isomer **17a** the two *o*-quinone moieties should be located in the cis position.

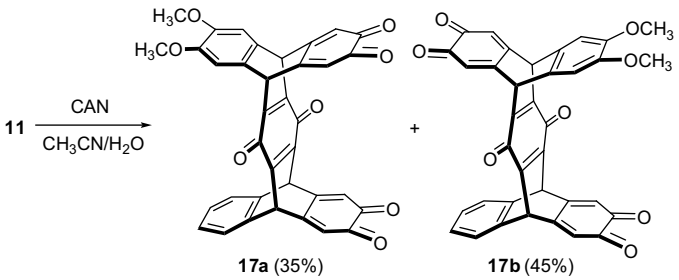

17a (35%) **17b** (45%)

Similarly, the isomers **18a** and **18b** were synthesized by the CAN oxidation of **12** in aqueous acetonitrile. The isomers could also be separated by column chromatography, but not be distinguished by ordinary spectroscopic methods. However, we could propose that the isomer **18b** with smaller polarity and poorer solubility has the two *o*-quinone moieties in the trans position, while **18a** has the two *o*-quinone moieties in the cis position.

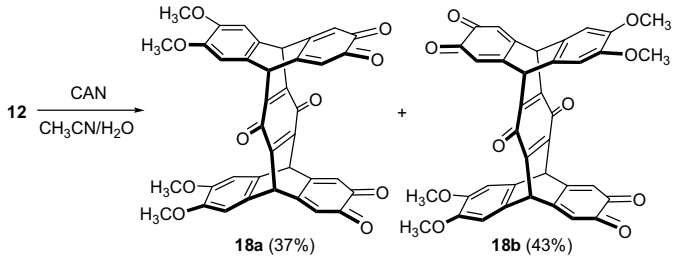

18a (37%) **18b** (43%)

2.3. Self-assemblies of pentiptycene quinones in the solid state

We have obtained the crystal structures of peripheral *o*-dimethoxy-substituted pentiptycene quinones **9**, **10a**, **10b**, and **12** with unique 3D rigid structure, and further studied their self-assemblies in the solid state. As shown in Figure 2a, the adjacent molecules of **9** with opposite orientation are alternately arranged to form two kinds of cavities, and in each cavity there are a couple of CH_2Cl_2 molecules. It was found that in one cavity there exists two pairs of C–Cl···π ($d_{C–Cl···π}$=3.445 Å for *f*, 3.357 Å for *g*) and one pair of C–H···Cl ($d_{C–H···Cl}$=2.937 Å for *h*) interactions between the CH_2Cl_2 molecules and their adjacent molecules of **9**. In the other cavity, one pair of C–Cl···π ($d_{C–Cl···π}$=3.319 Å for *l*) and one pair of C–H···O ($d_{C–H···O}$=2.566 Å for *k*) interactions between the CH_2Cl_2 molecules and their adjacent molecules of **9** were observed. By the linker of CH_2Cl_2 molecules, molecule **9** self-assembled into 1D supramolecular structure, which then formed a layer structure by the multiple non-covalent interactions between the adjacent molecules of **9** with the distances of 2.841 (a), 2.694 (b), 2.863 (c), 2.456 (d), 2.590 (e), and 2.889 Å (i). Moreover, a C–H···π interaction between the proton of dichloromethane and the aromatic ring of **9** with distance of 2.786 Å (j) was also shown. Furthermore, by packing of the adjacent layers, a 3D microporous structure viewed along the *b*-axis could be formed, and dichloromethane molecules were found to be located in the channels (Fig. 2b).

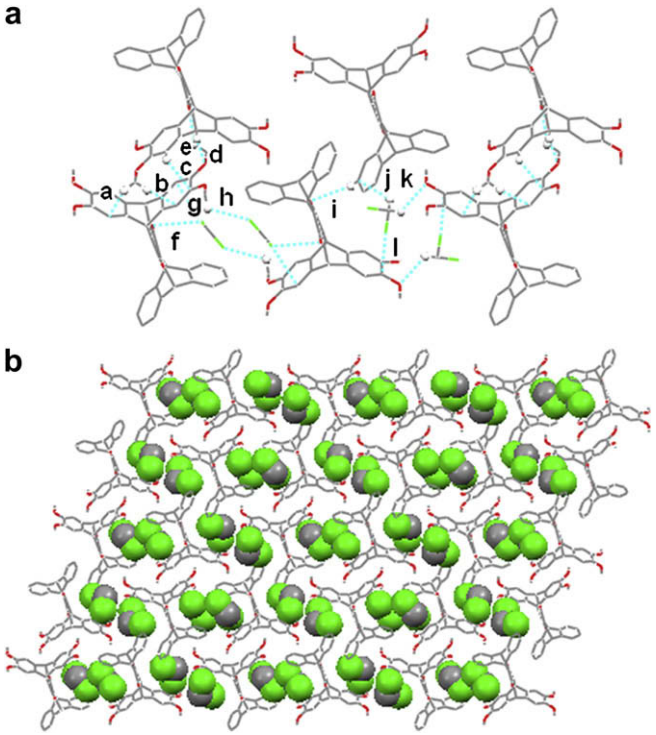

Figure 2. Packing of **9**. (a) View of multiple non-covalent interactions (dashed lines) between the adjacent molecules. (b) View of a 3D microporous structure with the CH_2Cl_2 located in the channels along the *b*-axis. Hydrogen atoms not involved in the interactions were omitted for clarity.

Similarly, compound **10a** could also self-assemble into a 3D microporous structure, in which there are two kinds of cavities in same size but opposite orientation (Fig. 3c). First, by virtue of two pairs of C–H···O hydrogen bonds ($d_{C–H···O}$=2.478 for a, 2.494 Å for b) between the oxygen atom of methoxy group in **10a** and the aromatic proton or bridgehead proton of its adjacent molecule, and two pairs of C–H···π ($d_{C–H···π}$=2.804 for c, 2.696 Å for d) interactions between the hydrogen atoms of the dimethoxybenzene moiety and the aromatic rings of its adjacent molecule (Fig. 3a), a layer structure could be formed. The adjacent layers then packed into a 3D microporous structure viewed along the *a*-axis by two pairs of C–H···O hydrogen bonding between the oxygen atom of the quinone moiety and the aryl proton and the bridgehead proton of the adjacent molecule with the distances of 2.595 (e) and 2.668 Å (f), respectively (Fig. 3b).

For molecule **10b**, it was found that in one layer four molecules could form a cavity by virtue of two pairs of C–H···O ($d_{C–H···O}$=2.501 for a, 2.501 Å for d) hydrogen bonds between the aromatic proton of one molecule and the methoxyl oxygen atom of its adjacent molecule, one pair of C–H···O ($d_{C–H···O}$=2.661 Å for f) hydrogen bond between the aromatic proton of one molecule and the quinoid oxygen atom of its adjacent molecule, and four pairs of C–H···π (for b and g, $d_{C–H···π}$=2.829 Å; for c and e, $d_{C–H···π}$=2.821 Å) interactions between the methyl proton of one molecule and the aromatic ring of its adjacent molecule (Fig. 4a). Moreover, it was found that the cavities in the adjacent layers took opposite orientation (Fig. 4b),

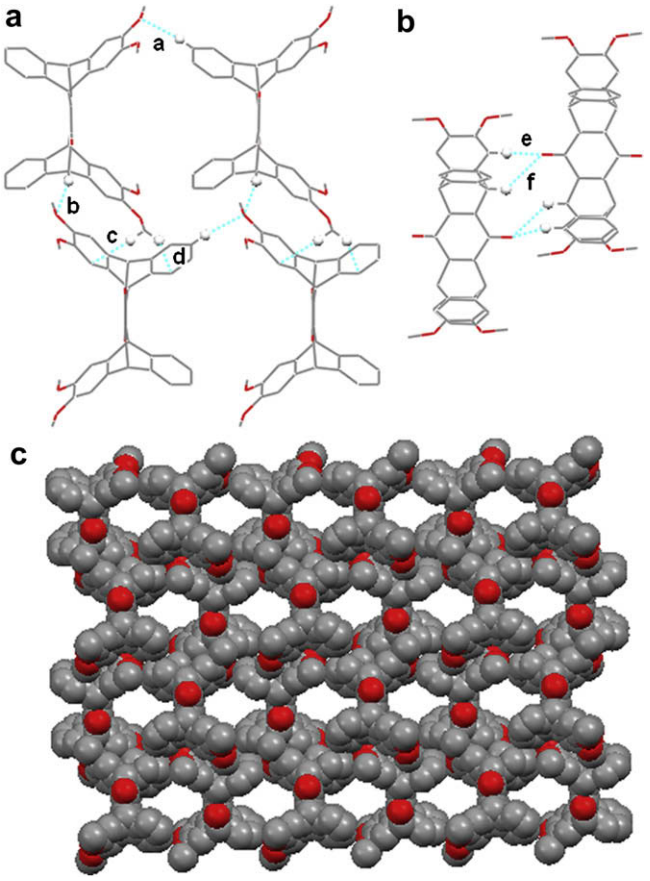

Figure 3. Packing of **10a**. (a) and (b) View of the non-covalent interactions (dashed lines) between the adjacent molecules. (c) View of a 3D microporous structure along the *a*-axis. Hydrogen atoms not involved in the interactions were omitted for clarity.

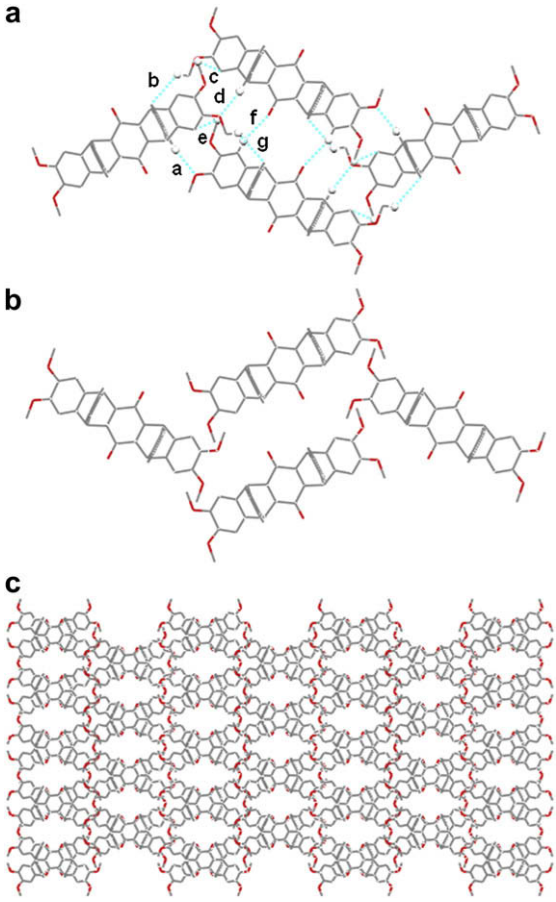

Figure 4. Packing of **10b**. (a) and (b) Two adjacent layers viewed along the *c*-axis. Blue dashed lines denote the non-covalent interactions between the adjacent molecules in a layer. (c) View of a 3D microporous structure along the *c*-axis. Hydrogen atoms not involved in the non-covalent interactions were omitted for clarity.

and the layers stake alternately in an AB sequence to result in a 3D microporous structure with the same cavity of nearly 11 Å in length and 5.6 Å in width (Fig. 4c).

In the case of **12**, each molecule was surrounded by eight other molecules, and every six molecules build up a cavity, which was stabilized by multiple non-covalent interactions. As shown in Figure 5a, there are two pairs of C–H···π interactions between the methoxyl protons of the central molecule and the aromatic rings of its adjacent molecules with the distances of 2.740 (a) and 2.877 Å (b), respectively. There also existed three pairs of C–H···O hydrogen bonding interactions between the oxygen atom of the central molecule and the aromatic protons and the bridgehead protons of its adjacent molecules with the distances of 2.648 (c), 2.579 (d), and 2.572 Å (e), respectively. Moreover, a pair of C–H···O hydrogen bonds between the oxygen atom of the quinone moiety and the aromatic proton of the adjacent molecule with the distance of 2.455 Å (f) were also shown (Fig. 5b). By virtue of these multiple non-covalent interactions, molecule **12** could self-assemble into a 3D microporous structure in the solid state, and $CHCl_3$ molecules were found to be located in the channels (Fig. 5c), which was similar to the case of **9**.

2.4. Photo-physical properties

The UV–vis absorption spectra of the pentiptycene quinones were carried out in $CHCl_3$ or CH_2Cl_2. Except compounds **7**, **13**, **14**, and **15**, all other pentiptycene quinones exhibited a distinct CT-absorption in the visible region, and the color[16] of the chloroform solution of the peripheral *o*-dimethoxy-substituted pentiptycene quinones changed from yellow to dark purple with

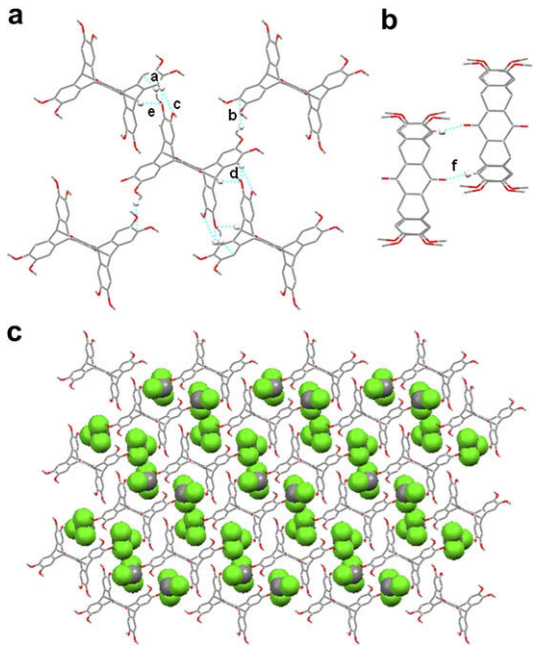

Figure 5. Packing of **12**. (a) and (b) View of the non-covalent interactions (blue dashed lines) between one molecule and its adjacent molecules. (c) View of a 3D microporous structure along the *b*-axis with $CHCl_3$ molecules located in the channels. Hydrogen atoms not involved in the interactions were omitted for clarity.

increasing number of catechol unit. These results might be attributed to the CT transition[13,17] for the symmetry-forbidden CT interaction between the electron donor of the catechol unit and the electron acceptor of the quinone unit fixed in the rigid framework. With increasing number of catechol unit, compounds **9**, **10a**, **10b**, **11**, and **12** displayed a progressive red shift of 7, 56, 64, 69 and 107 nm, respectively, compared with the CT band of **8** at 423 nm (Fig. 6, Table 1). Interestingly, it was found that although compounds **9**, **10a**, and **10b** all contain two catechol units, compared with **9**, compounds **10a** and **10b** displayed a red shift of 49 and 57 nm, respectively, which implied that position of the electron donor also played an important role in the intramolecular CT interaction. In the UV–vis spectra of pentiptycene derivatives **13**–**18** containing *o*-quinone, *p*-quinone and catechol units simultaneously, two distinct CT-absorption bands (Fig. 7) were observed. Moreover, it was also found that the contribution of the pentiptycene quinone **9** with DAD-type nonparallel 3D structure fixed in one of its triptycene moiety to CT band strength was less than that of compound **16** with ADA-type 3D structure. In the cases of **7**, **13**, **14**, and **15**, no apparent CT-bands but only characteristic absorption bands of the π–π* and n–π* transitions of the quinone moiety were observed, which might be due to the weak electron donor of the benzene ring. The results are consistent with those ones of the triptycene *o*-quinone derivatives.[18]

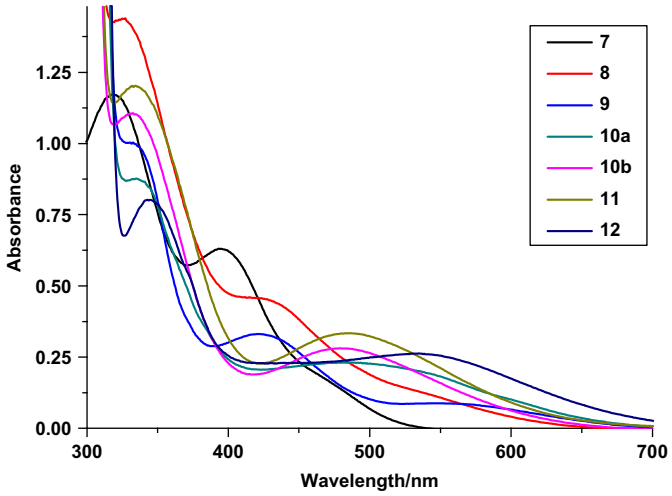

Figure 6. UV–vis absorption spectra of peripheral *o*-dimethoxy-substituted pentiptycene quinones in $CHCl_3$ (1.2×10^{-3} M).

Table 1
Summary of the physical property measurements of peripheral *o*-dimethoxy-substituted pentiptycene quinones and their *o*-quinone derivatives

Compound	λ_{CT} (nm)	log ε (dm³/mol)	$E_{1/2}$ (V)[a]
7[b]	—	—	−1.31
8[b]	423	2.58	−1.22
9[b]	430	2.43	−1.22
10a[b]	479	2.37	−1.24
10b[b]	487	2.44	−1.25
11[b]	492	2.29	−1.19
12[b]	530	2.34	−1.33
13[c]	—	—	−1.10, −1.37
14[c]	—	—	−0.88, −1.32
15[c]	—	—	−0.80, −1.19
16[c]	434, 583	3.90, 2.94	−1.00, −1.39
17a[c]	432, 583	3.64, 2.74	−0.87, −1.14, −1.26
17b[c]	—[d]	—[d]	—[d]
18a[c]	430, 583	3.91, 2.97	−0.85, −1.24
18b[c]	435, 584	3.91, 2.97	−0.87, −1.32

[a] Performed with a three-electrode system (platinum disk as working electrode, platinum rod as counter electrode, and Ag/Ag^+ as reference electrode) in $CHCl_3$ or CH_2Cl_2 containing 0.1 M $(NBu_4)NPF_6$ as supporting electrolyte at a scan rate of 0.1 V s^{-1}.
[b] The experiments were carried out in $CHCl_3$.
[c] The experiments were carried out in CH_2Cl_2.
[d] Poor solubility in CH_2Cl_2.

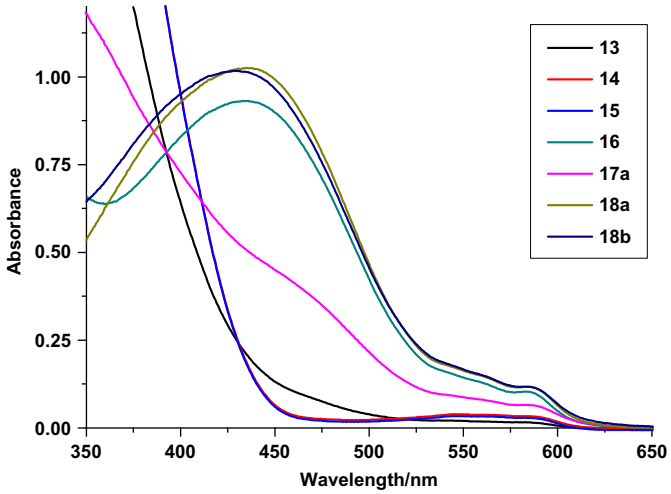

Figure 7. UV–vis absorption spectra of pentiptycene *o*-quinone derivatives in CH_2Cl_2 (1.2×10^{-4} M).

2.5. Electrochemical properties

We further evaluate the electrochemical properties of the pentiptycene quinones by cyclic voltammetry in $CHCl_3$ or CH_2Cl_2 with 0.1 M $(NBu_4)PF_6$ as the supporting electrolyte, and the results are summarized in Table 1. As shown in Figure 8, the CV curve of **8** exhibits one couple of cathodic and anodic peaks with the half-wave potential of −1.22 V, which is similar to those ones of the *p*-quinones, and consistent with a irreversible two-electron redox process.[19] Similar to compound **8**, other pentiptycene quinones bearing one *p*-benzoquinone moiety also showed one couple of irreversible cathodic and anodic peaks. Moreover, compared with **7** containing no *o*-dimethoxy groups, the half-wave potential of **8**, **9**, **10a**, **10b**, and **11** moved to less negative values,[16] suggesting that their quinone units were more easy to be reduced than that of **7**. However, for pentiptycene quinone **12** with the same D_{2h} symmetry of **7**, it was found that almost same half-wave potential values between **7** and **12** were shown (Table 1).

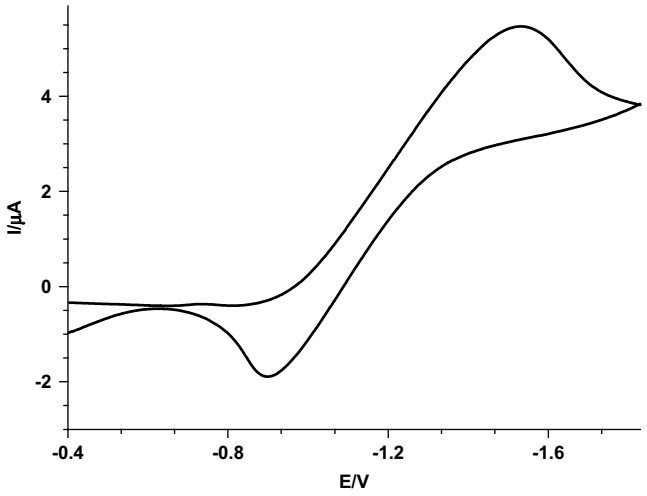

Figure 8. CV curve for compound **8** (1.2 mM) in $CHCl_3$ with $(NBu_4)PF_6$ (0.1 M) as the supporting electrolyte. Scan rate: 0.1 V s^{-1}.

As for the pentiptycene *o*-quinone derivatives **13** and **16** bearing one *p*-quinone moiety and one *o*-quinone moiety are concerned, two couples of cathodic and anodic peaks were expectedly observed.[16] The results suggested that each of the quinone moieties showed a two-electron redox process, and the *o*-quinone ring was more easily reduced when compared with the *p*-quinoid ring. In the case of **14** bearing one *p*-quinone moiety and two *o*-quinone moieties with the same chemical environment, two irreversible two-electron redox processes with the half-wave potential at −1.32 and −0.88 V, respectively, were only shown (Fig. 9). Similarly, **15**, **18a**, and **18b** also exhibited two irreversible two-electron redox processes, and the *p*-quinone unit was hard to be reduced compared with the *o*-quinone units. As for compound **17a** with the two *o*-quinone units in different chemical environment, three two-electron redox processes could be observed.[16]

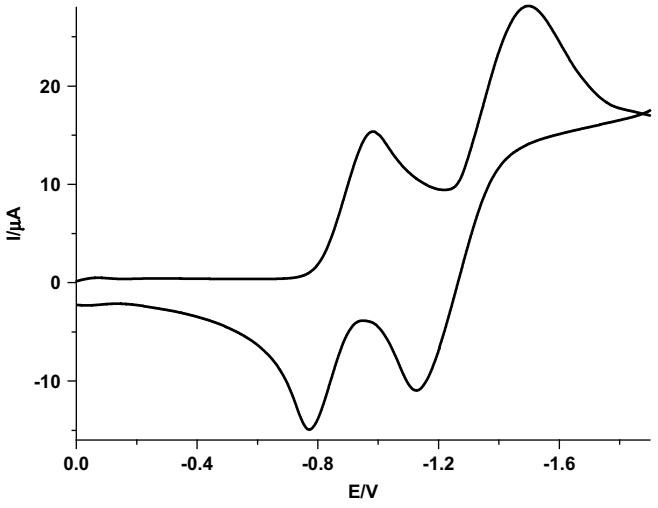

Figure 9. CV curve for compound **14** (1.2 mM) in CH_2Cl_2 with $(NBu_4)PF_6$ (0.1 M) as the supporting electrolyte. Scan rate: 0.1 V s^{-1}.

3. Conclusions

In conclusion, we have synthesized a series of peripheral *o*-dimethoxy-substituted pentiptycene quinones and their *o*-quinone derivatives, and found that one of the two *o*-dimethoxybenzene moieties situated at the same side of the pentiptycene quinones could be only oxidized by excess CAN in aqueous acetonitrile. We also found that the pentiptycene quinones with unique 3D rigid structure could all self-assemble into a 3D microporous structure in the solid state. Moreover, the pentiptycene quinones, especially the ones containing the *o*-dimethoxybenzene unit(s) and the quinone group(s) simultaneously, exhibited interesting intramolecular charge transfer interactions due to the symmetry-forbidden CT interaction between the electron donor of the catechol units and the electron acceptor of the quinone units fixed in the rigid framework, and also electrochemical properties. We believe that these peripheral-substituted pentiptycene quinones and their *o*-quinone derivatives will find wide applications in material science and host–guest chemistry,[9] just similar to the cases of triptycene derivatives.[20] Design and synthesis of novel hosts based these pentiptycene quinones as new building blocks are now underway in our laboratory.

4. Experimental

4.1. General

^1H and ^{13}C NMR spectra were recorded using a Bruker Spectrospin AV300 instrument. Tetramethylsilane (TMS) was used as an internal standard, with chemical shifts expressed in parts per million (ppm) downfield from the standard. Mass spectra were determined by MALDI-TOF technique. Elementary analyses were performed in the Analytic Laboratory of this Institute. Flash column chromatography was carried out with silica gel (100–200 mesh). Other reagents and solvents were purchased from common commercial sources, and were used as received or purified by distillation from appropriate drying agents.

*4.1.1. Compound **6**.* A mixture of 2,3,6,7-tetramethoxyanthracene (440 mg, 1.48 mmol) and *p*-benzoquinone (799 mg, 7.4 mmol) in acetic acid (100 mL) and 1,2-dichloroethane (25 mL) was refluxed for 3 days. The reaction mixture was concentrated under reduced pressure, resolved with CH_2Cl_2, washed by water for several times, and the organic layer was then dried over anhydrous sodium sulfate. The solvent was concentrated under reduced pressure, and the crude product was purified by column chromatography over silica gel (eluent: CH_2Cl_2 and then 50:1 v/v CH_2Cl_2/ethyl acetate) to give **6** (330 mg) in 55% yield as a dark-purple solid. Mp >300 °C. ^1H NMR (300 MHz, $CDCl_3$): δ 3.84 (s, 12H), 5.62 (s, 2H), 6.77 (s, 2H), 7.03 (s, 4H). ^{13}C NMR (75 MHz, $CDCl_3$): δ 46.7, 56.3, 109.0, 135.3, 136.8, 146.2, 153.3, 183.7. EIMS: *m*/*z* 404 $[M]^+$, 389 $[M-OCH_3]^+$, 374 $[M-2CH_3]^+$. Anal. Calcd for $C_{24}H_{20}O_6\cdot 1.5H_2O$: C, 66.81; H, 5.37. Found: C, 66.58; H, 5.02.

*4.1.2. Compound **7**.* A mixture of anthracene (3.56 g, 20 mmol), *p*-benzoquinone (1.08 g, 10 mmol), and *p*-chloranil (4.92 g, 20 mmol) in AcOH (120 mL) was refluxed for 16 h. The resulting mixture was cooled to room temperature. The precipitate was filtered, washed with ether, and then dried under reduced pressure to give 4.11 g (89%) of **7**[10] as a yellow solid.

*4.1.3. Compound **8**.* A mixture of 2,3-dimethoxyanthracene (0.476 g, 2 mmol), triptycene quinone **4** (0.568 g, 2 mmol), and *p*-chloranil (0.492 g, 2 mmol) in AcOH (50 mL) was refluxed for 16 h. The resulting mixture was cooled to room temperature. The precipitate was filtered, washed with ether, and then dried under reduced pressure to give 0.78 g (75%) of **8** as a light orange solid, which was further purified by column chromatography over silica gel with 3:1 (v/v) CH_2Cl_2/petroleum ether (60–90 °C) as the eluent. Mp >300 °C. ^1H NMR (300 MHz, $CDCl_3$): δ 3.79 (s, 6H), 5.67 (s, 2H), 5.75 (s, 2H), 6.91–7.04 (m, 8H), 7.31–7.37 (m, 6H). ^{13}C NMR (75 MHz, $CDCl_3$): δ 47.2, 47.5, 56.3, 109.4, 123.9, 124.2, 125.3, 125.5, 136.5, 143.7, 144.2, 146.5, 151.0, 151.7, 180.0. MALDI-TOF MS: *m*/*z* 520.2 $[M]^+$, 543.2 $[M+Na]^+$. Anal. Calcd for $C_{38}H_{28}O_6\cdot 1/5CH_2Cl_2$: C, 80.88; H, 4.58. Found: C, 80.70; H, 4.60.

*4.1.4. Compound **9**.* A mixture of **6** (40 mg, 0.1 mmol), anthracene (18 mg, 0.1 mmol), and *p*-chloranil (25 mg, 0.1 mmol) in AcOH (15 mL) was refluxed for 18 h. Workup as described for **6** yielded 51 mg (89%) of **9** as a dark-green solid. Mp >300 °C. ^1H NMR (300 MHz, $CDCl_3$): δ 3.79 (s, 12H), 5.59 (s, 2H), 5.75 (s, 2H), 6.94–6.99 (m, 8H), 7.35–7.37 (m, 4H). ^{13}C NMR (75 MHz, $CDCl_3$): δ 46.9, 47.5, 56.3, 109.3, 124.2, 125.5, 137.0, 143.7, 146.3, 150.9, 152.4, 180.1. MALDI-TOF MS: *m*/*z* 580.2 $[M]^+$, 603.2 $[M+Na]^+$. Anal. Calcd for $C_{38}H_{28}O_6\cdot 3/2H_2O$: C, 75.11; H, 5.14. Found: C, 75.32; H, 4.80.

*4.1.5. Compounds **10a**/**10b**.* A mixture of 2,3-dimethoxyanthracene (1.213 g, 5.1 mmol), *p*-benzoquinone (0.27 g, 2.5 mmol), and *p*-chloranil (1.24 g, 5.0 mmol) in AcOH (120 mL) was refluxed for 48 h. Workup as described for **6** yielded **10a** (0.62 g) in 42% yield and **10b** (0.64 g) in 43% yield as red purple solid, respectively. **10a**: Mp >300 °C. ^1H NMR (300 MHz, $CDCl_3$): δ 3.79 (s, 12H), 5.67 (s, 4H), 6.91–6.98 (m, 8H), 7.31–7.36 (m, 4H). ^{13}C NMR (75 MHz, $CDCl_3$): δ 47.2, 56.3, 109.4, 123.9, 125.3, 136.5, 144.2, 146.5, 151.6, 180.1.

MALDI-TOF MS: *m*/*z* 580.3 $[M]^+$, 603.2 $[M+Na]^+$. Anal. Calcd for $C_{38}H_{28}O_6 \cdot 3/4CH_2Cl_2$: C, 72.23; H, 4.61. Found: C, 72.26; H, 4.76. Compound **10b**: Mp >300 °C. ^{1}H NMR (300 MHz, $CDCl_3$): δ 3.79 (s, 12H), 5.67 (s, 4H), 6.91–6.98 (m, 8H), 7.31–7.36 (m, 4H). ^{13}C NMR (75 MHz, $CDCl_3$): δ 47.2, 56.3, 109.4, 123.9, 125.3, 136.5, 144.2, 146.5, 151.6, 180.1. MALDI-TOF MS: *m*/*z* 580.3 $[M]^+$, 603.2 $[M+Na]^+$. Anal. Calcd for $C_{38}H_{28}O_6 \cdot CH_2Cl_2$: C, 70.38; H, 4.54. Found: C, 69.99; H, 4.71.

*4.1.6. Compound **11**.* A mixture of **6** (100 mg, 0.25 mmol), anthracene (59 mg, 0.25 mmol), and *p*-chloranil (63 mg, 0.25 mmol) in AcOH (38 mL) was refluxed for 22 h. Workup as described for **6** yielded 120 mg (75%) of compound **11** as a dark-purple solid. Mp >300 °C. ^{1}H NMR (300 MHz, $CDCl_3$): δ 3.79 (s, 18H), 5.59 (s, 2H), 5.67 (s, 2H), 6.95–6.98 (m, 8H), 7.33–7.35 (m, 4H). ^{13}C NMR (75 MHz, $CDCl_3$): δ 46.9, 47.2, 53.3, 56.3, 109.3, 109.4, 123.9, 125.3, 136.5, 137.1, 144.2, 146.4, 146.5, 151.6, 152.3, 180.1. MALDI-TOF MS: *m*/*z* 640.2 $[M]^+$, 663.2 $[M+Na]^+$. Anal. Calcd for $C_{40}H_{32}O_8$: C, 74.99; H, 5.03. Found: C, 74.99; H, 5.47.

*4.1.7. Compound **12**.* A mixture of 2,3,6,7-tetramethoxy-anthracene (149 mg, 0.5 mmol), **6** (202 mg, 0.5 mmol), and *p*-chloranil (123 mg, 0.5 mmol) in acetic acid (100 mL) and 1,2-dichloroethane (25 mL) was refluxed for 8 days. Workup as described for **6** gave the crude product, which was further purified by column chromatography over silica gel (eluent: 50:1 v/v $CHCl_3$/ethyl acetate) to yield 56 mg (16%) of **12** as a dark-purple solid. Mp >300 °C. ^{1}H NMR (300 MHz, $CDCl_3$): δ 3.79 (s, 24H), 5.59 (s, 4H), 6.97 (s, 8H). ^{13}C NMR (75 MHz, $CDCl_3$): δ 46.9, 56.3, 109.0, 137.0, 146.2, 152.3, 180.2. MALDI-TOF MS: *m*/*z* 700.3 $[M]^+$, 723.3 $[M+Na]^+$. Anal. Calcd for $C_{42}H_{36}O_{10} \cdot 1.3CH_2Cl_2$: C, 60.76; H, 4.39. Found: C, 60.75; H, 4.31.

*4.1.8. Compound **13**.* A mixture of **8** (100 mg, 0.19 mmol) and CAN (313 mg, 0.57 mmol) in acetonitrile (15 mL) and water (5 mL) was stirred at room temperature for 6 h. The reaction mixture was extracted with CH_2Cl_2. The organic layer was dried over anhydrous sodium sulfate and then concentrated under reduced pressure. The crude product was further purified by column chromatography over silica gel with $CHCl_3$ as eluent to give **13** (89 mg) in 94% yield as a yellow solid. Mp >300 °C. ^{1}H NMR (300 MHz, $CDCl_3$): δ 5.49 (s, 2H), 5.82 (s, 2H), 6.33 (s, 2H), 7.00–7.05 (m, 6H), 7.38–7.43 (m, 6H). ^{13}C NMR (75 MHz, $CDCl_3$): δ 45.1, 47.5, 122.6, 124.4, 124.5, 125.1, 125.7, 128.6, 137.0, 143.3, 143.4, 144.3, 150.1, 152.2, 178.8, 178.9. MALDI-TOF MS: *m*/*z* 490.0 $[M]^+$, 513.0 $[M+Na]^+$. Anal. Calcd for $C_{34}H_{18}O_4 \cdot 0.3CHCl_3$: C, 78.27; H, 3.50. Found: C, 78.22; H, 3.77.

*4.1.9. Compound **14**.* A mixture of **10a** (200 mg, 0.34 mmol) and CAN (1.17 g, 2.14 mmol) in acetonitrile (30 mL) and water (8 mL) was stirred at room temperature for 10 h. The reaction mixture was extracted with CH_2Cl_2. The organic layer was dried over anhydrous sodium sulfate and then concentrated under reduced pressure. The crude product was further purified by column chromatography over silica gel with 200:1 (v/v) CH_2Cl_2/CH_3OH as eluent to give **14** (170 mg) in 94% yield as an orange solid. Mp >300 °C. ^{1}H NMR (300 MHz, $CDCl_3$): δ 5.50 (s, 4H), 6.41 (s, 4H), 7.28–7.32 (m, 4H), 7.42–7.45 (m, 4H). ^{13}C NMR (75 MHz, DMSO): δ 38.7, 44.1, 122.7, 125.1, 127.9, 137.6, 144.7, 149.9, 179.0, 179.1. MALDI-TOF MS: *m*/*z* 543.8 $[M+Na]^+$. Anal. Calcd for $C_{34}H_{16}O_6 \cdot 0.4CH_2Cl_2$: C, 74.52; H, 3.05. Found: C, 74.33; H, 3.08.

*4.1.10. Compound **15**.* A mixture of **10b** (580 mg, 1 mmol) and CAN (3.29 g, 6 mmol) in acetonitrile (70 mL) and water (10 mL) was stirred at room temperature for 6 h. Workup as described for **14** gave compound **15** (438 mg) in 84% yield as an orange solid. Mp >300 °C. ^{1}H NMR (300 MHz, $CDCl_3$): δ 5.50 (s, 4H), 6.36 (s, 4H), 7.32–7.35 (m, 4H), 7.47–7.50 (m, 4H). MALDI-TOF MS: *m*/*z* 543.8 $[M+Na]^+$. Anal. Calcd for $C_{34}H_{16}O_6 \cdot 1.7CH_2Cl_2$: C, 64.49; H, 2.94. Found: C, 64.26; H, 2.81.

*4.1.11. Compound **16**.* A mixture of **9** (100 mg, 0.17 mmol) and CAN (567 mg, 1.03 mmol) in acetonitrile (20 mL) and water (5 mL) was stirred at room temperature for 6 h. Workup as described for **13** gave the crude product, which was further purified by column chromatography over silica gel with 30:1 (v/v) CH_2Cl_2/ethyl acetate as eluent to yield **16** (75 mg) in 80% yield as a red solid. Mp >300 °C. ^{1}H NMR (300 MHz, $CDCl_3$): δ 3.85 (s, 6H), 5.35 (s, 2H), 5.82 (s, 2H), 6.32 (s, 2H), 6.93–7.05 (m, 6H), 7.36–7.43 (m, 4H). ^{13}C NMR (75 MHz, $CDCl_3$): δ 44.8, 47.6, 56.3, 108.8, 121.9, 124.4, 124.5, 125.6, 125.7, 129.2, 143.3, 143.4, 144.8, 149.8, 149.9, 152.2, 178.9, 179.1. MALDI-TOF MS: *m*/*z* 550.9 $[M]^+$. Anal. Calcd for $C_{36}H_{22}O_6$: C, 78.54; H, 4.03. Found: C, 78.65; H, 4.36.

*4.1.12. Compounds **17a**/**17b**.* A mixture of **11** (100 mg, 0.16 mmol) and CAN (849 mg, 1.44 mmol) in acetonitrile (30 mL) and water (6 mL) was stirred at room temperature for 3 h. Workup as described for **13** gave the crude product, which was further purified by column chromatography over silica gel with 20:1 (v/v) CH_2Cl_2/ethyl acetate as eluent to yield **17a** (42 mg) in 45% yield and **17b** (32 mg) in 35% yield as red solids. **17a**: Mp >300 °C. ^{1}H NMR (300 MHz, $CDCl_3$): δ 3.87 (s, 6H), 5.42 (s, 2H), 5.51 (s, 2H), 6.37 (s, 2H), 6.41 (s, 2H), 6.95 (s, 2H), 7.42–7.45 (m, 4H). ^{1}H NMR (300 MHz, DMSO): δ 3.78 (s, 6H), 5.56 (s, 2H), 5.66 (s, 2H), 6.42 (s, 2H), 6.50 (s, 2H), 7.19 (s, 2H), 7.25–7.35 (m, 2H), 7.48–7.61 (m, 2H). ^{13}C NMR (75 MHz, $CDCl_3$): δ 44.9, 45.2, 56.4, 108.7, 122.3, 123.0, 125.3, 125.4, 128.8, 136.8, 145.5, 145.9, 149.6, 149.8, 149.9, 178.0, 178.8, 179.0. MALDI-TOF MS: *m*/*z* 584.2 $[M+4]^+$. Anal. Calcd for $C_{36}H_{20}O_8$: C, 74.48; H, 3.47. Found: C, 74.61; H, 3.20. Compound **17b**: Mp >300 °C. ^{1}H NMR (300 MHz, $CDCl_3$): δ 3.88 (s, 6H), 5.42 (s, 2H), 5.48 (s, 2H), 6.37 (s, 2H), 6.41 (s, 2H), 6.96 (s, 2H), 7.42–7.44 (m, 4H). MALDI-TOF MS: *m*/*z* 584.3 $[M+4]^+$, 603.3 $[M+Na]^+$. Anal. Calcd for $C_{36}H_{20}O_8$: C, 74.48; H, 3.47. Found: C, 74.75; H, 3.80.

*4.1.13. Compounds **18a**/**18b**.* A mixture of **12** (70 mg, 0.10 mmol) and CAN (658 mg, 1.20 mmol) in acetonitrile (30 mL) and water (6 mL) was stirred at room temperature for 3 h. Workup as described above gave **18a** (24 mg) in 37% yield and **18b** (40 mg) in 43% yield as red solids. Compound **18a**: Mp >300 °C. ^{1}H NMR (300 MHz, $CDCl_3$): δ 3.87 (s, 12H), 5.41 (s, 4H), 6.35 (s, 4H), 6.99 (s, 4H). ^{1}H NMR (300 MHz, DMSO): δ 3.72 (s, 12H), 5.55 (s, 4H), 6.42 (s, 4H), 7.19 (s, 4H). ^{13}C NMR (75 MHz, DMSO): δ 43.7, 55.9, 109.4, 121.8, 129.5, 145.2, 148.8, 150.0, 178.1, 179.3. MALDI-TOF MS: *m*/*z* 646.4 $[M+2]^+$. Anal. Calcd for $C_{38}H_{24}O_{10}$: C, 71.25; H, 3.78. Found: C, 71.05; H, 4.02. Compound **18b**: Mp >300 °C. ^{1}H NMR (300 MHz, $CDCl_3$): δ 3.88 (s, 12H), 5.42 (s, 4H), 6.37 (s, 4H), 6.99 (s, 4H). MALDI-TOF MS: *m*/*z* 640.3 $[M]^+$. Anal. Calcd for $C_{38}H_{24}O_{10}$: C, 71.25; H, 3.78. Found: C, 71.62; H, 3.98.

4.2. Crystal data

CCDC 735920 (**9**), CCDC 735921 (**10a**), CCDC 735922 (**10b**), and CCDC 735923 (**12**) contain the supplementary crystallographic data for this paper. These data can be obtained free of charge from The Cambridge Crystallographic Data Centre via www.ccdc.cam.ac.uk.

*4.2.1. Crystal data for **9**·2CH_2Cl_2.* $C_{40}H_{32}Cl_4O_6$, M_w=750.46, crystal size 0.12×0.10×0.04 mm^3, monoclinic, space group *P* 2(1)/*n*, *a*=18.713(4) Å, *b*=8.4043(17) Å, *c*=23.334(5) Å, α=90°, β=108.36 (3)°, γ=90°, *U*=3483.1(12) Å^3, *Z*=4, D_c=1.431 Mg/m^3, *T*=113(2) K, μ=0.389 mm^{-1}, 22,540 reflections measured, 6027 unique

(R_{int}=0.2844), final R indices [$I>2\sigma(I)$]: R_1=0.1286, wR_2=0.2440, R indices (all data): R_1=0.2470, wR_2=0.2837.

4.2.2. Crystal data for ***10a****.* $C_{38}H_{28}O_6$, M_w=580.60, crystal size 0.19×0.17×0.13 mm^3, orthorhombic, space group *Pbcn*, a=8.2020 (16) Å, b=20.714(4) Å, c=21.656(4) Å, α=90°, β=90°, γ=90°, U=3679.4(13) Å^3, Z=4, D_c=1.048 Mg/m^3, T=173(2) K, μ=0.071 mm^{-1}, 21,384 reflections measured, 3419 unique (R_{int}=0.0461), final R indices [$I>2\sigma(I)$]: R_1=0.0583, wR_2=0.1475, R indices (all data): R_1=0.0656, wR_2=0.1520.

4.2.3. Crystal data for ***10b****.* $C_{38}H_{28}O_6$, M_w=580.60, crystal size 0.47×0.28×0.23 mm^3, monoclinic, space group C 2/c, a=26.511(5) Å, b=8.3967(17) Å, c=16.199(3) Å, α=90°, β=121.57(3)°, γ=90°, U=3072.5(11) Å^3, Z=4, D_c=1.255 Mg/m^3, T=173(2) K, μ=0.085 mm^{-1}, 5068 reflections measured, 2704 unique (R_{int}=0.0250), final R indices [$I>2\sigma(I)$]: R_1=0.0618, wR_2=0.1666, R indices (all data): R_1=0.0776, wR_2=0.1720.

4.2.4. Crystal data for 0.5 ***12****·2CHCl$_3$.* $C_{22}H_{19}Cl_3O_5$, M_w=469.72, crystal size 0.18×0.04×0.02 mm^3, monoclinic, space group $P2(1)/n$, a=15.504(3) Å, b=8.2128(16) Å, c=18.047(4) Å, α=90°, β=99.26(3)°, γ=90°, U=2267.9(8) Å^3, Z=4, D_c=1.376 Mg/m^3, T=113(2) K, μ=0.434 mm^{-1}, 14,887 reflections measured, 3989 unique (R_{int}=0.0864), final R indices [$I>2\sigma(I)$]: R_1=0.0727, wR_2=0.2054, R indices (all data): R_1=0.1065, wR_2=0.2378.

Acknowledgements

We thank the National Natural Science Foundation of China (20532030, 20625206, 20772126), the National Basic Research Program (2007CB808004, 2008CB617501), and the Chinese Academy of Sciences for financial support. We also thank Dr. H.B. Song at Nankai University, Dr. X. Hao and Ms T.L. Liang at Institute of Chemistry, CAS for determining the crystal structures.

Supplementary data

Color changes of pentiptycene quinones **7**–**12**. Copies of cyclic voltammetry (CV) curves of the pentiptycene quinones. Supplementary data associated with this article can be found, in the online version, at doi:10.1016/j.tet.2009.07.090.

References and notes

1. (a) Hart, H.; Shamouilian, S.; Takehira, Y. *J. Org. Chem.* **1981**, *46*, 4427–4432; (b) Yang, J.-S.; Yan, J.-L. *Chem. Commun.* **2008**, 1501–1512.
2. (a) Yang, J.-S.; Swager, T. M. *J. Am. Chem. Soc.* **1998**, *120*, 5321–5322; (b) Yang, J.-S.; Swager, T. M. *J. Am. Chem. Soc.* **1998**, *120*, 11864–11873.
3. Zyryanov, G. V.; Palacios, M. A.; Anzenbacher, P., Jr. *Org. Lett.* **2008**, *10*, 3681–3684.
4. Yang, J.-S.; Lin, C.-S.; Hwang, C.-Y. *Org. Lett.* **2001**, *3*, 889–892.
5. Yang, J.-S.; Lee, C.-C.; Yau, S.-L.; Chang, C.-C. *J. Org. Chem.* **2000**, *65*, 871–877.
6. Yang, J.-S.; Huang, Y.-T.; Ho, J.-H.; Sun, W.-T.; Huang, H.-H.; Lin, Y.-C.; Huang, S.-J.; Huang, S.-L.; Lu, H.-F.; Chao, I. *Org. Lett.* **2008**, *10*, 2279–2282.
7. (a) Wiehe, A.; Senge, M. O.; Kurreck, H. *Liebigs Ann. Recl.* **1997**, 1951–1963; (b) Wiehe, A.; Senge, M. O.; Schafer, A.; Speck, M.; Tannert, S.; Kurreck, H.; Roder, B. *Tetrahedron* **2001**, *57*, 10089–10110.
8. Yang, J.-S.; Liu, C.-P.; Lee, G.-H. *Tetrahedron Lett.* **2000**, *41*, 7911–7915.
9. Cao, J.; Jiang, Y.; Zhao, J.-M.; Chen, C.-F. *Chem. Commun.* **2009**, 1987–1989.
10. (a) Clar, E. *Ber. Dtsch. Chem. Ges.* **1931**, *64*, 1676–1687; (b) Theilacker, W.; Berger-Brose, U.; Beyer, K.-H. *Chem. Ber.* **1960**, *93*, 1658–1681.
11. Zhu, X.-Z.; Chen, C.-F. *J. Org. Chem.* **2005**, *70*, 917–924.
12. Bartlett, P. D.; Ryan, M. J.; Cohen, S. G. *J. Am. Chem. Soc.* **1942**, *64*, 2649–2653.
13. Yamamura, K.; Nakasuji, K.; Murata, I.; Inagaki, S. *J. Chem. Soc., Chem. Commun.* **1982**, 396–397.
14. (a) Miao, Q.; Nguyen, T. Q.; Someya, T.; Blenchet, G. B.; Nuckolls, C. *J. Am. Chem. Soc.* **1942**, *64*, 2649–2653; (b) Danielsen, K.; Francis, G. W.; Aksnes, D. W. *Magn. Reson. Chem.* **1996**, *34*, 1043–1047; (c) Pozzo, J.-L.; Clavier, G. M.; Colomes, M.; Bouas-Laurent, H. *Tetrahedron* **1997**, *53*, 7377–7390.
15. Jacob, P.; Callery, P. S.; Shulgin, A. T.; Castagoli, N., Jr. *J. Org. Chem.* **1976**, *41*, 3627–3629.
16. See Supplementary data.
17. (a) Iwamura, H.; Makino, H. *J. Chem. Soc., Chem. Commun.* **1978**, 720–721; (b) Murata, I. *Pure Appl. Chem.* **1983**, *55*, 323–330; (c) Norvez, S.; Barzoukas, M. *Chem. Phys. Lett.* **1990**, *165*, 41–44; (d) Nobuya, K. *Bull. Chem. Soc. Jpn.* **1989**, *62*, 800–807.
18. Zhao, J.-M.; Lu, H.-Y.; Cao, J.; Jiang, Y.; Chen, C.-F. *Tetrahedron Lett.* **2009**, *50*, 219–222.
19. Chambers, J. Q. In *The Chemistry of the Quinonoid Compounds*; Patai, S., Ed.; Wiley: New York, NY, 1974; pp 737–792.
20. (a) Zhu, X.-Z.; Chen, C.-F. *J. Am. Chem. Soc.* **2005**, *127*, 13158–13159; (b) Zong, Q.-S.; Chen, C.-F. *Org. Lett.* **2006**, *8*, 211–214; (c) Han, T.; Chen, C.-F. *Org. Lett.* **2006**, *8*, 1069–1072; (d) Peng, X.-X.; Lu, H.-Y.; Han, T.; Chen, C.-F. *Org. Lett.* **2007**, *9*, 895–898; (e) Zhao, J.-M.; Zong, Q.-S.; Han, T.; Xiang, J.-F.; Chen, C.-F. *J. Org. Chem.* **2008**, *73*, 6800–6806.